Information Sciences 219 (2013) 168–180

Contents lists available at SciVerse ScienceDirect

Information Sciences

journal homepage: www.elsevier.com/locate/ins

Texture analysis and classification: A complex network-based approach

André Ricardo Backes [a], Dalcimar Casanova [b], Odemir Martinez Bruno [b,]*

[a] Universidade Federal de Uberlândia, Faculdade de Computação, Brazil
[b] Universidade de São Paulo, Instituto de Física de São Carlos, Brazil

ARTICLE INFO

Article history:
Received 9 November 2010
Received in revised form 3 July 2012
Accepted 14 July 2012
Available online 24 July 2012

Keywords:
Texture analysis
Texture recognition
Complex network

ABSTRACT

In this paper, we propose a novel texture analysis method using the complex network theory. We investigated how a texture image can be effectively represented, characterized and analyzed in terms of a complex network. The proposed approach uses degree measurements to compose a set of texture descriptors. The results show that the method is very robust, and it presents a excellent texture discrimination for all considered classes, overcoming traditional texture methods.

1. Introduction

Texture analysis is a basic issue in image processing and computer vision. It is a key problem in many application areas, such as object recognition, remote sensing, and content-based image retrieval. Even though there is no exact definition for the term texture [55], this is an attribute easily comprehended by humans, and it is a wealthy source of visual information (when considering the tri-dimensional nature of physical objects). The importance of texture perception in human vision is one of the early steps towards identifying objects and understanding a scene. Many efforts have been made to understand these mechanisms throughout the years. Some recent results can be seen in [38,52]. In fact, the visual mechanism has inspired many models of object recognition used today in computer vision. Recent reports from both neuroscience and computer vision have demonstrated that biologically plausible features [27,31,53] are attractive in visual recognition.

Biological inspired methods in computer vision started becoming well-known at the beginning of the 1980s. David Marr's book [40] played a significant role in its popularization. Since then, neurological primate brain models have lead to the development of many computer vision methods. On the other hand, biological models have made it easier to understand Mathematics based on visual attributes. Taking this into account, many mathematical methods without biological inspiration have also been proposed, which is the case of the method proposed here. It is not directly involved with biological inspired methods, but makes use of Pattern Recognition and Computer Vision concepts that were enhanced by neuroscience advances. According to [55], an image texture is defined as a function of spatial variation in pixel intensities (gray values). This definition is useful in a variety of applications and is the subject of this research. Basically, a texture pattern can have many or few texture primitives (micro-textures) and/or hierarchic spatial arrangements of these primitives (macro-texture). The textural perception of an image depends on the spatial size of these primitives. Large primitives give rise to macro-texture (i.e. coarse texture) and small primitive to micro-texture (i.e. fine texture).

Due to this characteristic, the definition of a texture class must take into account not only the isolated primitives, but also the relation among them and their neighbors. Taking this into account, Julesz [36] shows that two textures are not

* Corresponding author.
E-mail addresses: backes@facom.ufu.br (A.R. Backes), dalcimar@gmail.com (D. Casanova), bruno@ifsc.usp.br (O.M. Bruno).

0020-0255/$ - see front matter © 2012 Elsevier Inc. All rights reserved.
http://dx.doi.org/10.1016/j.ins.2012.07.003

discriminative by human vision if their second order statistics are identical. Consequently, texture characterization and identification require a methodology which is able to express the context surrounding each pixel, therefore joining local and global texture characteristics. It should be mentioned that there is a growing body of literature on texture characterization. It can be divided into four [42,24,55] major categories: statistical, geometrical, model-based and signal processing methods. Good reviews of traditional methods can be found in [48,55,26,59,41,46].

This paper proposes a novel approach to represent and characterize the relation among structural elements of texture using the Complex Networks Theory. To accomplish this task, texture should be represented as a complex network, including the information about image pixels and their neighbors to the vertices and edges, followed by an analysis of the topological features of the computed network [21]. These features may be used to distinguish different classes of images. Experimental results are compared with traditional texture methods such as First-order features, Fourier descriptors, Gabor filters, GLCM, DCT, GLDM, Wavelets descriptors, CLBP, LBPV and LTP.

The paper is organized as follows. Section 2 gives a brief review of the Complex Network Theory, as well as its properties and the proposed modeling from a texture to a complex network. Section 3 shows the process of computing a network signature for the modeled texture. The method is evaluated in Section 4. In Section 5 the results are presented and discussed. In Section 6, conclusions of the work are drawn.

2. Complex network

Complex networks are natural structures, which represent many real-world systems. Recently, there has been much interest from various fields of science concerning the study of statistical properties of such networks [1,43,15]. Even though many topics of computer vision can be modeled using complex network techniques, this is still an unexplored field and there are few references in the literature [7,6,25,5,20]. Research concerning Complex Networks can be defined as the intersection between graph theory and statistical mechanisms, which confers a truly multidisciplinary nature to this area [21]. The first studies of this theory can be seen in Flory [22], Rapoport [49–51] and Erdös and Rényi [16–18].

One of the main reasons why complex networks have become so popular is their flexibility and generality in representing virtually any natural structure, including those undergoing dynamic changes of topology [21]. As a matter of fact, every discrete structure such as lists, trees, networks and images [20] can be suitably represented as a graph. Taking this into account, various studies include investigations on how to represent a problem as a complex network, followed by an analysis of its topological characteristics and feature extraction. Some applications use these descriptors to distinguish different classes, and therefore create techniques for pattern recognition [33].

Many papers representing real structures as complex networks exist in the literature. In Refs. [2,3], complex networks are used for modeling texts. The results of some experiments have shown that there is a strong correlation between the network's parameters and the text quality. In Ref. [10], the problem of texture characterization is presented in terms of complex networks: the image pixels are represented as nodes and similarities between such pixels are mapped as links between the network nodes. It can be observed that various types of textures present node degree distributions, which are very distinct from those observed in random networks, thus suggesting a complex organization of those textures. Traditional measurements of network connectivity are then applied in order to obtain feature vectors, which can be used for texture characterization and classification.

The idea of this work is similar to the above related work and it focuses on pattern recognition of texture. Due to its importance to human communication, representing and analyzing images in terms of graphs and complex networks offers a promising (and challenging) research opportunity in forthcoming years.

2.1. Texture as a pixel network

Texture is defined as a bi-dimensional structure of pixels. In gray-scale images, each pixel is characterized by an integer value $g = 0, \ldots, L$, which represents the intensity of light in that pixel, where L is the maximum number of gray-levels in the image. Let $I(x,y) = g, x = 1, \ldots, M$ and $y = 1, \ldots, N$, be a pixel in an image I, where x and y are the Cartesian coordinates of the pixel $I(x,y)$. A graph $G = (V,E)$ is built by considering each pixel $I(x,y)$ of the image I as a vertice $v_{x,y} \in V$ of the graph G (see Fig. 1a). The vertices associated to two pixels $I(x,y)$ and $I(x',y')$ are connected by a non-directed edge $e \in E,\ e = (v_{x,y}, v_{x',y'})$, when the Euclidean distance between them is no longer than a value r (see Fig. 1b):

$$E = \left\{ e = (v_{x,y}, v_{x',y'}) \in I \times I | \sqrt{(x-y')^2 + (x-y')^2} \leqslant r \right\}. \tag{1}$$

For each non-directed edge $e \in E$ we associate a weight $w(e)$, which is defined by the square of the Euclidean distance between the two connected vertices and the difference of pixel intensity between $I(x,y)$ and $I(x',y')$, normalized according to the square of the radius r (see Fig. 1c):

$$w(e) = (x-x')^2 + (y-y')^2 + r^2 \frac{|I(x,y) - I(x',y')|}{L} \quad \forall e = (v_{x,y}, v_{x',y'}) \in E. \tag{2}$$

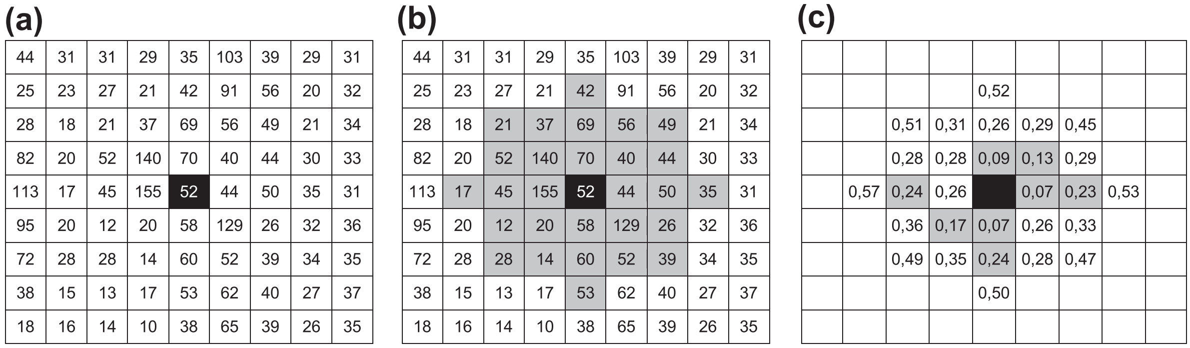

Fig. 1. Texture as pixel network: (a) each pixel of the image is a vertice in the graph; (b) two vertices are connected if the Euclidean distance between them is no longer than a r value (gray pixels for $r = 3$ in this example); and (c) a weight defined by Eq. (3) is associated to all connected vertices. A threshold t is applied to the original set of edges ($t = 0.25$, in this example) to perform a transformation in the network, thus resulting in a subset of edges (gray pixels).

This approach enables us to include context information about pixel surroundings, which refers to a local texture analysis. Moreover, the normalization of the difference of pixel intensity in the interval $[0,r^2]$ ensures that both geometric and color information have equal importance in the texture characterization. By considering that the connection between the two pixels depends on parameter r, which is associated to the covering radius of a pixel in the image, the weight function $w(e)$ may assume a very large range of values. Thus, it is interesting to normalize the weight $w(e)$ in the interval $[0,1]$. This is performed by using the largest value possible in a connection. This value corresponds to the sum of the normalized maximum difference of intensity between two pixels, r^2, and the square of the maximum distance allowed between them, r^2:

$$w(e) = \frac{(x-x')^2 + (y-y')^2 + r^2\,\frac{|I(x,y)-I(x',y')|}{L}}{r^2+r^2} \quad \forall e = (v_{x,y}, v_{x',y'}) \in E. \tag{3}$$

Note that, initially, each network vertice presents a similar number of connections. Therefore, the computed graph presents a regular behavior. However, a regular graph is not considered a complex network, and it does not present any relevant property for the proposed application. Thus, it is necessary to transform this graph into a complex network that has relevant properties for texture analysis. This transformation and network properties are discussed in the following sections.

2.2. Histogram degree

The *degree* (or *connectivity*) of a node v, $deg(v)$, represents the number of edges connected to v, i.e., the number of neighbors of v. Be $\partial v = \{v' \in V | (v,v') \in E\}$, the set of neighbors of v, the degree of a node v is defined as:

$$deg(v) = |\{e \in E | v \in e\}| = |\{v' \in V | \{v, v'\} \in E\}| = |\partial v|, \tag{4}$$

where $|A|$ denotes the cardinality (number of elements) of a set A [58]. Equivalently, we may define $deg(v)$ as the number of edges incident in v. By computing the degree for each network vertice $v \in V$, the histogram degree h is achieved as

$$h(i) = \sum_{v \in V} \delta(deg(v), i), \tag{5}$$

where $\delta(j,i)$ is the Kronecker's delta

$$\delta(j,i) = \begin{cases} 1, & j = i, \\ 0, & j \neq i. \end{cases} \tag{6}$$

The histogram is obviously a simple and concise source of statistical information of the network topology. Many features can be computed by analyzing of the degree histogram. These features are, basically, first-order statistics, and they are computed from the probability density function $p(i)$ of the histogram $h(i)$, which is yielded as:

$$p(i) = \frac{h(i)}{\sum_{i=0}^{k} h(i)} \quad i = 0, 1, \ldots, k. \tag{7}$$

where $k = \max_{v \in V} deg(v)$ is the maximum degree of graph G.

For network characterization using degree histogram analysis, the following set of features were evaluated:

Mean:

$$\mu = \sum_{i=0}^{k} i p(i) \tag{8}$$

Contrast:

$$C = \sum_{i=0}^{k} p(i) i^2 \tag{9}$$

Energy:

$$E = \sum_{i=0}^{k} [P(i)^2] \tag{10}$$

Entropy:

$$H = -\sum_{i=0}^{k} p(i) \log_2 [p(i)] \tag{11}$$

The first two features are the mean and contrast of vertices degrees within the network. The energy and entropy are also computed. The energy is useful to examine the power content (repeated transitions) in a certain frequency band. Entropy is a common concept in many fields, mainly in signal processing, and it describes the uniformity of degree distribution [12]. Note that such features are particularly relevant for texture characterization as they provide a good compromise between local (i.e., degree measurements centered at each image pixel and influenced by neighbor pixels) and global (i.e., histograms) information.

3. Complex network texture signature

In the previous section, we focused on the static properties of a network. We showed that some features computed from the degree histogram can be used to characterize both local and global characteristics of the network. However, in real systems, a network characterization cannot be fully complete without considering the interplay between structural and dynamic aspects [8].

Modeling the dynamics of a complex network is a difficult task, as different networks may present a large range of characteristics [8]. An interesting approach to extract additional information about the structure and dynamic of a complex network is to apply a transformation to the original network and then compute the properties of the network obtained [21]. There are many possibilities carry out this transformation. A simple way is to apply a threshold t to the original set of edges E, thus selecting a subset E_t, $E_t \subseteq E$, where each edge of $e \in E_t$ has weight $w(e)$ equal to or smaller than t (see Fig. 1c). From this new set of edges E_t and the original set of vertices V, a new network $G_t = (V, E_t)$ arises, which represents an intermediary stage in the network evolution. This transformation is represented as

$$E^* = \delta_t(E) = \{e \in E | w(e) \leqslant t\}. \tag{12}$$

Thus, by applying a set of thresholds T, $t \in T$, to the original network G, it is possible to study the behavior of its histogram features previously discussed, such as the mean, energy, entropy and contrast (Fig. 2). This process can also be interpreted as the acquisition of various samplings of a complex network throughout its life (from creation to extinction). This approach grants us a signature which contains temporary characteristics of the network and, therefore, a richer set of measurements that describes the network behavior:

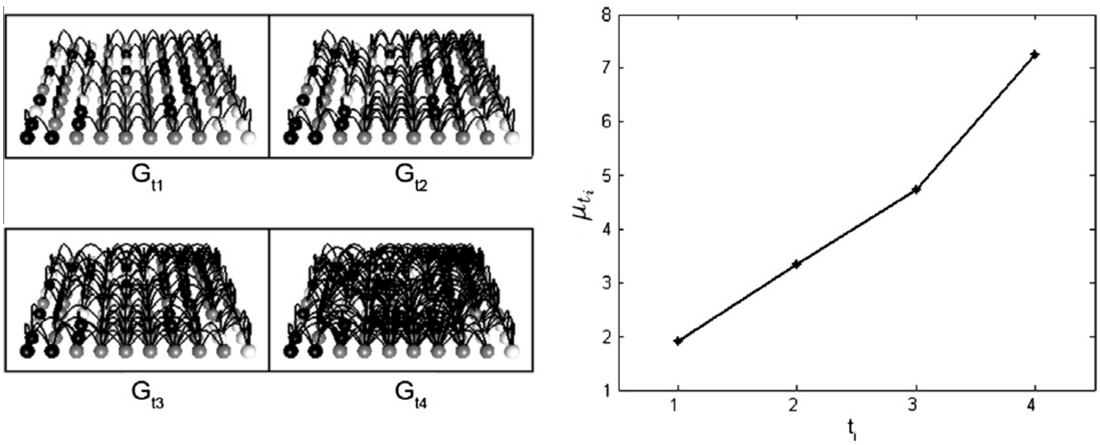

Fig. 2. Left: a texture example modeled as a Complex network, different threshold values ($t_1 \cdots t_4$) make different topological features. Right: complex network characterization by its evolution (mean degree at each threshold t_i.

$$\varphi = [\mu_{t_1}, \ldots, \mu_{t_M}], \; t_i \in T, \tag{13}$$

where μ_{t_i} is the mean of the degree histogram computed from the network achieved for a threshold t_i. Fig. 3 shows two complex networks computed from different textures using the same threshold value.

At first, our method may look similar to the GLDM (Gray Level Difference Matrix) and GLCM (Gray Level Co-occurrence Matrix) methods. Both methods use the gray level differences as the basis to characterize the texture, but in different ways. The GLCM method considers the number of pixels with the same intensity, at a specific distance and angle. The GLDM method considers the difference between pixel intensity at a specific distance and angle. Our method does not differentiate distance or angle between pixels. Our method considers as a characteristic the edge weight, or, in other words, the energy necessary to change its states from a dark to a bright pixel in another position. Therefore, the conjecture of Julesz is not applicable here, because we are not calculating second order statistics, as GLCM does.

4. Evaluation

In order to evaluate the proposed method, the signatures were calculated for different configurations and used in a texture analysis context. The three image databases used in this evaluation:

- Brodatz texture album [9]: A database with 1776 texture samples grouped into 111 classes was used. Each image is 128×128 pixels with 256 gray levels.
- The VisTex color textures [56]: The Vision Texture (VisTex) database maintained by the Vision and Modelling group at the MIT Media Lab. The full database contains images representative of real-world textures in practical conditions (lighting, perspective, etc.). In this work, we use 54 gray-scale VisTex images of 512×512 resolution. They were split into 16 non-overlapping sub-images of 128×128.
- The suite Outex_TC_00013: Provided by Outex texture database [45]. This database includes a collection of natural scenes. The test suite provides meaningful entities for the empirical evaluation of a candidate texture analysis algorithm. A database of 1360 gray-scale texture images (128×128) was constructed by splitting each one of the 68 original texture images (746×538) into 20 non-overlapping sub-images.

To evaluate properties of rotation invariance of the method, an additional database was built by rotating each sample of the first database by a specific angle. Fig. 4 shows examples of a given texture at different rotation angles.

In addition, we ran some experiments on robustness against noise. For each image in the 3 databases we added gaussian white noise of mean 0 and variance 0.01. We also added salt and pepper noise that affected approximately 0.05% of the pixels. Fig. 5 shows both effects in the sample images.

4.1. Linear discriminant analysis

Signatures computed from each texture sample were evaluated using statistical analysis. This analysis was carried out by applying a Linear Discriminant Analysis (LDA) (also called Fisher linear discriminant) to the data in a leave-one-out cross-validation scheme. LDA is a well known method for estimating a linear subspace with good discriminative properties. The idea of this method is to find data where the variance between the classes is large in comparison to the variance within the classes. The LDA method also enables us to verify the cluster's distribution in feature space. A descriptor is considered "good" when it creates compact clusters far away from each other for all classes in the corresponding feature space. As it is a supervised method, the LDA needs class definitions for the estimation process [19,23].

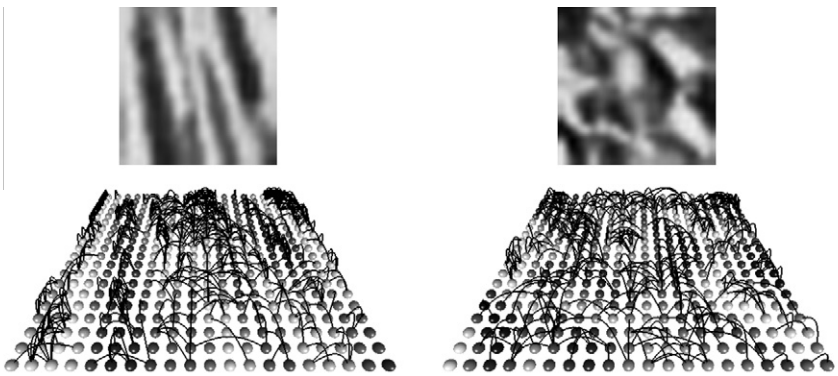

Fig. 3. Two complex networks, at same threshold value, for two different texture samples. The differences in their topological features results in measurements which can be used as texture descriptors.

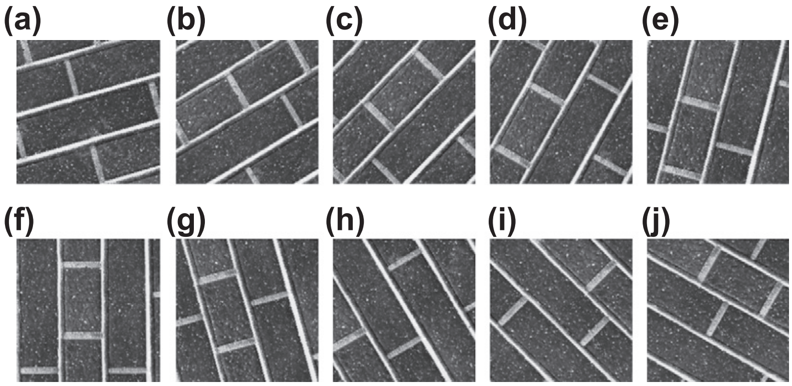

Fig. 4. Example of Brodatz rotated samples: (a) 15°; (b) 30°; (c) 45°; (d) 60°; (e) 75°; (f) 90°; (g) 105°; (h) 120°; (i) 135°; and (j) 150°.

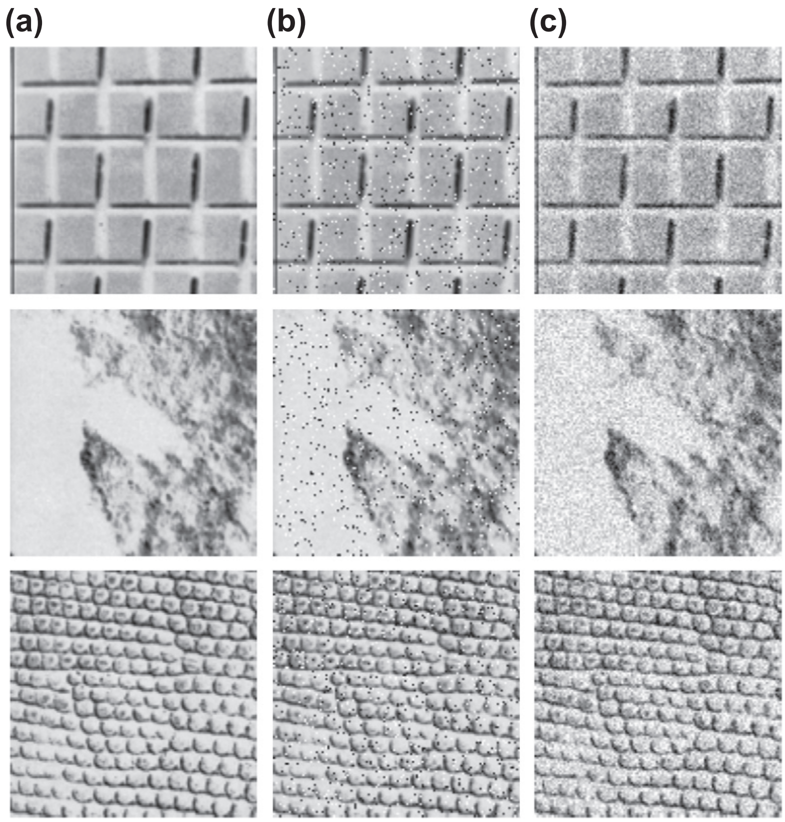

Fig. 5. Samples of Brodatz images with gaussian and salt and pepper noise. (a) Original images; (b) salt and pepper noise; and (c) Gaussian noise.

4.2. Experiments

The results were compared with other traditional descriptors found in the literature. These descriptors are: First-order histogram [41], Fourier descriptors [4], Gabor filters [39,34,14,32], Gray Level Co-occurrence Matrix [30], Discrete Cosine Transform (DCT) [44], Gray Level Difference Matrix (GLDM)[57,37], Wavelets descriptors [13,11,48,35], Local Binary Pattern Variance (LBPV) [29], Complete Local Binary Pattern (CLBP) [28] and Local Ternary Pattern (LTP) [54].

- First-order histogram based features: Mean, variance, kurtosis, energy and entropy features are extracted from the image's histogram, totaling 5 descriptors.

- Fourier descriptors: Fourier transform is applied to the texture sample and a feature vector producing energy of the 64 coefficients is computed. The Fourier bi-dimensional spectrum is divided into 64 sectors with eight radial distances and eight angles (after performing a *shifting* operation). Each feature corresponds to the sum of the spectrum absolute values of each sector.
- Gabor filters: The 2-D Gabor filter is basically a bi-dimensional gaussian function moduled with an oriented sinusoid in a determined frequency and direction. This procedure consists of convolving an input image by a family of Gabor filters, which present various scales and orientations of the same original configuration. Out of the numerous tests performed, we achieved the best results using a family of 64 filters (8 rotation filter and 8 scale filters), with a lower and upper frequency equal to 0.01 and 0.4, respectively. The definition of the individual parameters of each filter follows the mathematical model presented in [39].
- Gray Level Co-occurrence Matrix (GLCM): Basically, this is the joint probability distribution between pairs of pixels at a determined distance and direction. For this comparison, distances of 1 and 2 pixels with angles of $-45°$, $-90°$, $45°$ and $90°$ were used. Contrast, correlation, energy and homogeneity measures were computed from resulting matrices, totaling a set of 32 descriptors. A non-symmetric version was adopted in the experiments.
- Discrete Cosine Transform (DCT): A set of eight 3×3 DCT masks is generated from three 1D DCT basis vectors $U_1 = 1,1,1^T$, $U_2 = 1,0,-1^T$, and $U_3 = 1,-2,1^T$. Nine masks can be produced from these vectors. We excluded the mask with low pass property. Then, we computed the local variance for each filter output.
- Gray Level Difference Matrix (GLDM): This is based on the occurrence of two pixels which have a given absolute difference in the gray level and separated by a specific intersample spacing d. In our experiment, we considered the distances $(0,d)$, $(-d,d)$, $(d,0)$, and $(-d,-d)$. Three intersample spacings (1, 2 and 5) and five measurements (contrast, angular second moment, entropy, mean, and inverse difference moment) were extracted from the estimated probability–density function, totaling 60 features.
- Wavelet descriptors: We used the multilevel 2D wavelet decomposition the in experiment. We carried out four dyadic decompositions using daubechies 4. We measured the energy, entropy and mean for horizontal, diagonal and vertical details, totaling 36 features.
- Complete Local Binary Pattern (CLBP): This is a new scheme of traditional LBP [47,60] descriptors. It uses the local difference sign-magnitude to build CLBP_C, CLBP_S and CLBP_M operators. These three operators can be combined in different ways. Here, we calculated a joint 3D histogram, denoted in the original article as CLBP_S/M/C. Additionally, we used *radius* = 2, *neighborhood* = 16 with rotation invariant uniform patterns $U \leqslant 2$ (riu2) totaling 648 features. The proposed nearest neighborhood classifier with the chi-square distance is used a classifier.
- Local Binary Pattern Variance (LBPV): This is a modified scheme of traditional LBP [47] descriptor that uses the rotation invariant measurement of the local variance. We set the *radius* = 3, *neighborhood* = 24 using uniform patterns, totaling 555 features. These are the best parameters in the author's paper for Outex database. We also used global matching using 2 main orientations for each image in the classification task.
- Local Ternary Pattern (LTP): This is another extension of the original LBP [47] operator that uses a 3-valued code in which the near graylevels of the neighbors to the central pixel are set to 0. The threshold used was 0.1, as suggested by the authors, with *radius* = 2, *neighborhood* = 8 totaling 32,768 features. We also used the proposed distance transform as a classifier.

For GLCM, DCT, GLDM, Wavelets and the proposed method, we used the LDA classifier using the leave-one-out cross-validation scheme. In the experiments, we reduced the original features into principal components, after the LDA projection, which represent 99.99% of the total variance. For the CLPB, LBPV and LTP methods we used the classifiers proposed by the authors.

5. Results and discussion

5.1. Parameter evaluation

The proposed approach suggests that features computed from degree histograms might be able to perform texture discrimination. However, to compute such features, we must first model the texture as a complex network using radius r. Then, we must apply a set of thresholds T to this network in order to compute different samples of the network throughout its life. From each sub-network, we use degree histograms to compute a set of desirable features. Based on the description of this method, we note that both radius r and the set of thresholds T are important parameters to be configured, and therefore, it is necessary to evaluate the behavior of the method should be evaluated concerning different configurations of these parameters.

We start by analyzing the behavior of the method for different threshold sets using a constant radius $r = 2$ in the Brodatz database. Table 1 summarizes the results for 10 different configurations of thresholds ($F1, F2, \ldots, F10$). To compose each set of thresholds T, we considered an initial threshold ($T_{initial}$), which is gradually increased by a value T_{incr}, until it achieves a maximum threshold (T_{final}). For each histogram achieved, we computed the energy feature for the classification of the texture database. Besides the success rate (which refers to the amount of textures correctly classified by the method) and the parameter values used for composing the feature vectors, Table 1 also shows the number of features used (i.e., number of thresholds).

Initially, we split the range of thresholds into three distinct intervals ($F1$, $F2$ and $F3$), all using the same T_{incr} value. We performed this test in order to verify the intervals of thresholds which concentrate the most meaningful information about the topological structure of the network, and therefore, of the texture. This comparison among threshold intervals showed that the most relevant texture information is found for thresholds $t < 0.640$. Having values higher than this, the method is barely capable of texture classification. The initial interval of thresholds $F1$ holds the main information about the texture pattern, followed by set $F2$. As the threshold selects edges from the network whose weights are smaller than its value, and the edge weight is a function which depends on the pixel gray-level, this result indicates that small and average changes in the gray-levels are more interesting for texture discrimination in the proposed method. Furthermore, abrupt changes in the gray-levels may indicate the presence of noise in the texture analyzed.

From these results, we decided to increase the increment (T_{incr}) used to define each threshold set previously described. Increments $T_{incr} = 0.010$ and $T_{incr} = 0.015$ were evaluated. Configurations from $F4$ to $F9$ present the results for this test. It can be observed that there was a small increase in the success rate for $T_{incr} = 0.010$ ($F4$, $F5$ and $F6$). This increase was followed by a decrease in the number of descriptors used, which are now half the number of descriptors previously used. This reduction in the number of descriptors indicates the presence of redundant features in the descriptors computed for $T_{incr} = 0.005$, and that the discarding of such descriptors improve the performance of the method, thus yielding a better discrimination. Note that this improvement in the success rate is even more significant in the third interval of thresholds ($F6$). As we kept raising the increment ($T_{incr} = 0.015$, configurations $F7$, $F8$ and $F9$), a new reduction in the number of descriptors occured, but now followed by a small decrease in the success rate (exception is made for set $F9$). This reduction in the success rate may indicate that a limit in the threshold increment was reached, and that important features may be discarded if this process continues. To compensate for this small decrease in the success rate, we decided to evaluate a new interval of thresholds ($F10$), which now joins the interval defined in $F7$ and half of the interval used in $F8$. This new configuration shows a higher texture discrimination power compared to all intervals evaluated up to this point and an intermediary number of descriptors.

As the best threshold set was defined, we decided to investigate the influence of the radius value r used to model the network. Table 2 presents the results yielded for different radius values and the threshold set $F10$, from Table 1. As in the previous experiment, energy features were computed from the histograms achieved and used to classify the Brodatz database. We noted that there was no meaningful improvement in the performance when the radius was increased from $r = 2$ to $r = 3$. However, for $r \geqslant 4$ we noted a sharp decrease in the success rate. A higher r value is able to model a more dense network, i.e., more vertices can be connected to each other. This fact seems to hinder the capacity of discrimination of the method, as it expands the local investigation of the texture pattern by enlarging the neighborhood which a vertice can examine.

As the final evaluation of the method's parameters, we decided to evaluate the discrimination power of each degree histogram's feature considered. We also evaluated different combinations of these features. For this experiment, we considered the best configuration of the parameters previously tested. Thus, in this experiment, we used a radius $r = 3$ and a threshold set T consisting of an initial threshold $T_{initial} = 0.005$, which was gradually increased by a value $T_{incr} = 0.015$, until it achieved a maximum threshold $T_{final} = 0.530$. Table 3 shows the results yielded for each feature combination.

Results show that, individually, entropy and energy features are the ones with higher capacity to discriminate a complex network and, as a consequence, texture patterns. This is not a surprise, as these features are extensively used in the study of probability distributions. However, the combination of these two features does not lead to the best results when the different features are combined two-by-two. In fact, the result of these two features combined is the worst of such combinations. This may indicate a partial inhibition of the discrimination power of one feature by the other. In this case, the best results are achieved when entropy is combined with one of the remaining features (contrast and mean, respectively).

We achieved the best results when three features were combined, more specifically, energy, entropy and contrast. We also noted that, in this type of combination, the presence of the entropy feature was more relevant than the energy, as the absence of this feature was characterized by the lower success rate. It is important to emphasize that combining different features also increases the number of descriptors used in the classification. In the best result achieved, we used a total of 108 features (36 for each different feature considered).

Table 1
Result for the proposed method for different thresholds set. Using $r = 2$ and energy feature for the Brodatz database.

Set	Thresholds			No. of descriptors	Success rate (%)
	$T_{initial}$	T_{incr}	T_{final}		
F1	0.005	0.005	0.320	64	86.77
F2	0.325	0.005	0.640	64	78.66
F3	0.645	0.005	0.950	62	27.81
F4	0.005	0.010	0.315	32	86.94
F5	0.325	0.010	0.635	32	78.88
F6	0.645	0.010	0.945	31	33.67
F7	0.005	0.015	0.320	22	85.92
F8	0.325	0.015	0.640	22	77.98
F9	0.645	0.015	0.945	21	35.81
F10	0.005	0.015	0.530	36	89.75

Table 2
Result for the proposed method for different radius values. Using energy feature for the Brodatz database.

Radius	Thresholds			No. of descriptors	Success rate (%)
	$T_{initial}$	T_{incr}	T_{final}		
2	0.005	0.015	0.530	36	89.75
3	0.005	0.015	0.530	36	89.86
4	0.005	0.015	0.530	36	88.46
5	0.005	0.015	0.530	36	85.30

Table 3
Results for different histogram features and their combination. For the Brodatz database using the best configuration defined in Table 2.

Combined Features				No. of descriptors	Success rate (%)
Energy	Entropy	Contrast	Mean		
X				36	89.86
	X			36	91.89
		X		36	89.47
			X	36	88.40
X	X			72	93.13
X		X		72	93.75
X			X	72	93.81
	X	X		72	94.93
	X		X	72	94.71
		X	X	72	93.69
X	X	X		108	95.27
X	X		X	108	95.21
X		X	X	108	94.43
	X	X	X	108	95.15

Although we found the best parameters for the Brodatz database, these same parameters attained good results in Outex and Vistex databases (see next section). We believe that for any given dataset, the initial intervals with a radius close to 3 will also achieve good results. This can be observed from the tables above, that show results close to the best for parameters with small changes.

5.2. Comparison with other methods

For comparison purposes, we compared our proposed method with traditional texture analysis methods described in Section 4.2. For this comparison, we considered three texture databases: Brodatz, Outex and Vistex. Since Outex and Vistex present color information in their texture samples, we considered only the luminance information to create their gray-scale versions. Table 4 presents the results achieved for each method, including our proposed approach using its best configuration for different texture databases. As in the previous experiments, results refer to the amount of textures correctly classified by each method. These databases are hard to classify, and cannot be distinguished by their gray levels alone, as first order features results showed.

Findings showed that the proposed method presents a higher success rate for all databases considered when compared with traditional texture analysis methods. This indicates that degree distribution features might be more related to the texture aspect and its "'roughness'" than the compared methods. However, it is important to note that the proposed approach uses more descriptors than some of the compared approaches to achieve these results. This is a concern, as methods such as GLDM presented a success rate close to ours using only 60 descriptors.

However, it must be emphasize that the results presented in Table 4 are for the best configuration of the method. Take as an example the use of only entropy features as shown in Table 3. In the case considered, a success rate of 91.89% is achieved for the Brodatz database using only 36 descriptors. This result presents a reduced number of descriptors and still performs better than the compared approaches (the exception is made only to GLDM and CLBP methods). Nevertheless, it is interesting to recall the results achieved when using entropy and contrast features. In this case, although the number of descriptors used will be slightly higher than by the GLDM method, its success rate is higher (94.93%), which corroborates the effectiveness of the approach for texture analysis and classification.

5.3. Rotation invariance

Besides the characteristics already discussed concerning the configuration of the method and its comparison with other existent approaches, this section also presents the results concerning the rotation invariance of the method. This is an interesting and desirable characteristic in texture recognition applications.

Table 4
Comparison of the proposed method with traditional texture analysis methods. High discrimination in all databases.

Method	No. of descriptors	Success rate (%)		
		Brodatz	Outex	Vistex
First Order	5	34.29	52.86	50.11
Fourier	64	84.34	84.48	92.59
Gabor	64	84.45	80.00	91.66
GLCM	32	90.76	83.45	94.56
DCT	8	77.19	63.52	78.47
GLDM	60	94.36	86.47	96.99
Wavelets	36	85.64	78.45	89.69
CLBP	648	95.32	85.80	98.03
LBPV	555	86.26	75.66	88.65
LTP	32,768	88.04	79.16	91.56
Proposed approach	108	95.27	86.76	98.03

Table 5 shows the results achieved for each method when it was applied to the rotated texture databases. Although we obtained good results, the proposed method was not better than the LBP based methods (i.e. CLBP, LBPV and LTP). LBP based methods perform a circular bit-wise right shift (i.e., rotating the neighbor set clockwise as many times as necessary for the maximum number of the most significant bits to be set to 0) in order to remove the effect of rotation, formally defined as *riu2* (rotation invariance uniform patterns) [29].

It is important to notice, that the rotation invariance is intrinsic in the proposed method as it does not use any special transformation to achieve a rotation invariance. The network model is derived from the Euclidean distance between pixels and, in discrete space a small error is added because the Eucledian distance is not constant at all rotation angles.

We also considered the intensity of the pixel as information to compose the edge weight in Eq. (2). Its value does not change during image rotation and, in association with the normalization step, it diminishes the rotation error created by the Eucledian distance, making the proposed method relatively invariant to the rotation.

5.4. Robustness against noise

To model a network from a texture pattern, our proposed method relies on the difference of nearby pixel intensity. Thus, it is important to evaluate its tolerance to noise. Tables 6 and 7 present the results achieved for each method compared in all databases corrupted by gaussian white noise (mean 0 and variance 0.01) and salt and pepper noise (0.05%), respectively.

The presence of noise affects the way the edges are built in the network. These changes in the network structure modify its inner characteristics, such as its transitivity, and as a consequence, the measurements computed to characterize the texture. As a result, we clearly noticed a decrease in the success rate of our method. However, we also observed that our method presented higher tolerance to salt pepper noise than gaussian white noise. This result was expected as the salt pepper noise affects a smaller amount of pixels of the texture in comparison with the gaussian white noise. We observed that our method obtained the best and second best results in the databases corrupted by the salt pepper noise. The same performance does not occur when gaussian white noise is used, but it is still competitive in Vistex and Brodatz databases.

5.5. Computational complexity

To model the texture pattern as a complex network, we considered each pixel as a node in the network. Considering an image of $N \times N$ size, this leads to N^2 nodes. Initially, each node is connected to all other nodes whose Euclidean distance is

Table 5
Comparison of the proposed method with traditional texture analysis methods using rotated textures.

Method	No. of descriptors	Success rate (%)		
		Brodatz	Outex	Vistex
First order	5	72.56	75.40	80.30
Fourier	64	88.04	82.62	90.74
Gabor	64	77.96	65.77	89.22
GLCM	32	90.41	76.60	94.61
DCT	8	53.97	54.01	70.70
GLDM	60	94.51	83.28	99.49
Wavelets	36	83.53	69.25	88.72
CLBP	648	99.18	97.59	99.49
LBPV	555	98.11	89.83	98.48
LTP	32,768	98.03	94.59	98.11
Proposed approach	108	94.59	85.56	98.48

Table 6
Comparison of the proposed method with traditional texture analysis methods using gaussian noise.

Method	No. of descriptors	Success rate (%)		
		Brodatz	Outex	Vistex
First order	5	35.36	39.92	51.96
Fourier	64	84.68	74.70	89.93
Gabor	64	82.20	60.00	89.23
GLCM	32	85.19	49.33	88.07
DCT	8	73.98	34.19	75.23
GLDM	60	90.14	51.54	92.93
Wavelets	36	77.75	42.79	81.59
CLBP	648	90.09	38.82	92.59
LBPV	555	83.78	29.63	79.16
LTP	32768	85.56	34.39	86.32
Proposed approach	108	85.81	36.91	88.19

Table 7
Comparison of the proposed method with traditional texture analysis methods using salt and pepper noise.

Method	No. of descriptors	Success rate (%)		
		Brodatz	Outex	Vistex
First order	5	37.72	52.86	54.05
Fourier	64	82.93	70.07	87.84
Gabor	64	81.47	57.35	88.54
GLCM	32	90.87	79.11	94.56
DCT	8	69.87	27.42	69.32
GLDM	60	93.75	86.32	96.87
Wavelets	36	81.64	52.27	83.21
CLBP	648	95.72	85.00	98.14
LBPV	555	84.79	64.92	87.93
LTP	32768	85.19	76.60	94.44
Proposed approach	108	94.93	86.69	97.33

Table 8
Running time achieved for all methods.

Method	Time (s)
First order	0.006
Fourier	0.072
Gabor	0.254
GLCM	0.034
DCT	0.021
GLDM	0.204
Wavelets	0.024
CLBP	0.544
LBPV	0.272
LTP	0.011
Proposed approach	0.087

smaller than a radius r. To accomplish this task, we must visit all nodes inside a $(2r+1) \times (2r+1)$ window for each node. This leads to a $(2r+1) \times (2r+1) \times N^2$ operations to build the network. Then, a total of threshold L is applied to the network to measure its inner characteristics. This results in a computational complexity $O((2r+1) \times (2r+1) \times N^2 \times L)$. However, parameters r and L are usually small in comparison with the number of nodes of the network (e.g., the best result of the method used $r = 3$ and $L = 36$). Thus, it is possible to affirm that the computational complexity of the method is $O(N^2)$. To provide a better evaluation of the method, Table 8 shows the running time for each method compared. We implemented all methods on a PC using Intel (R) Core (TM) i7 Q720 CPU @ 1.60Ghz, 4 GB RAM, 64-bit Operating System and Matlab 7.9 64-bit. Time results indicate that, even though our approach does not have the lowest time, its running time is very competitive.

6. Conclusion

In this paper, we proposed a novel method of texture analysis using the complex network theory. We investigated how a texture image can be effectively represented, characterized and analyzed in terms of a complex network. Results showed that the method is very robust as it presented an excellent texture discrimination for all texture databases considered, outdoing traditional texture analysis methods. Moreover, the method was also tolerant to rotation variance of the texture. The compromise between local and global properties and the interplay between structural and dynamical aspects can provide valuable information about the structure being analyzed. Concerning the Complex Network Theory, the success in texture discrimination demonstrates the potential of the application of this approach in computer vision problems and digital image processing.

Acknowledgments

Odemir M. Bruno gratefully acknowledges the financial support from CNPq (National Council for Scientific and Technological Development, Brazil) (Grant #308449/2010-0 and #473893/2010-0) and FAPESP (The State of São Paulo Research Foundation) (Grant #2011/01523-1). André R. Backes is grateful to FAPESP (Proc. #06/54367-9) for his doctorate grant. Dalcimar Casanova is grateful to FAPESP (Proc. #08/57313–2) for his doctorate grant.

References

[1] R. Albert, A. Barabási, Statistical mechanics of complex networks, Reviews of Modern Physics 74 (2002) 47–97.
[2] L. Antiqueira, M. das Gracas V. Nunes, O.N.O. Junior, L. da F. Costa, Strong correlations between text quality and complex networks features, Physica A 373 (2007) 811–820.
[3] L. Antiqueira, O.N.O. Jr., L. da F. Costa, M. das Gratas Volpe Nunes, A complex network approach to text summarization, Information Sciences 179 (2009) 584–599.
[4] R. Azencott, J.P. Wang, L. Younes, Texture classification using windowed fourier filters, IEEE Transactions on Pattern Analysis and Machine Intelligence 19 (1997) 148–153.
[5] A.R. Backes, O.M. Bruno, A graph-based approach for shape skeleton analysis, Lecture Notes in Computer Science, vol. 5716, Springer, Berlin, Heidelberg, 2009.
[6] A.R. Backes, O.M. Bruno, Shape classification using complex network and multi-scale fractal dimension, Pattern Recognition Letters 31 (2010) 44–51.
[7] A.R. Backes, D. Casanova, O.M. Bruno, A complex network-based approach for boundary shape analysis, Pattern Recognition 42 (2009) 54–67.
[8] S. Boccaletti, V. Latora, Y. Moreno, M. Chavez, D.U. Hwang, Complex networks: structure and dynamics, Physics Reports 424 (2006) 175–308.
[9] P. Brodatz, Textures: A Photographic Album for Artists and Designers, Dover Publications, 1966.
[10] F.M.T. Chalumeau, L. da F. Costa, O. Laligant, Texture discrimination using hierarchical complex networks, in: Proceedings of the Second International Conference on Signal-Image Technology and Internet-Based Systems, pp. 543–550.
[11] T. Chang, C.C. Kuo, Texture analysis and classification with tree-structure wavelet transform, IEEE Transactions on Image Processing 2 (1993) 429–441.
[12] R.R. Coifman, M.V. Wickerhauser, Entropy-based algorithms for best basis selection, in: IEEE Transactions on Information Theory, pp. 713–718.
[13] I. Daubechies, Ten Lectures on Wavelets, Society for Industrial and Applied Mathematics, 1992.
[14] J. Daugman, C. Downing, Gabor wavelets for statistical pattern recognition, in: M.A. Arbib (Ed.), The Handbook of Brain Theory and Neural Networks, MIT Press, 1995, pp. 414–419.
[15] S.N. Dorogovtsev, J.F.F. Mendes, Evolution of Networks: From Biological Nets to the Internet and WWW, Oxford University Press, 2003.
[16] P. Erdös, A. Rényi, On random graphs, I, Publicationes Mathematicae 6 (1959) 290–297.
[17] P. Erdös, A. Rényi, On the evolution of random graphs, in: Publication of the Mathematical Institute of the Hungarian Academy of Sciences, pp. 17–61.
[18] P. Erdös, A. Rényi, On the strength of connectedness of a random graph, Acta Mathematica Scientia Hungary 12 (1961) 261–267.
[19] B.S. Everitt, G. Dunn, Applied Multivariate Analysis, Arnold, 2001.
[20] L. da F. Costa, Complex Networks, Simple Vision, 2004.
[21] L.daF. Costa, F.A. Rodrigues, G. Travieso, P.R. Villas Boas, Characterization of complex networks: a survey of measurements, Advances in Physics 56 (2007) 167–242.
[22] P.J. Flory, Molecular size distribution in three-dimensional polymers, Journal of the American Chemical Society 63 (1941) 3083–3090.
[23] K. Fukunaga, Introduction to Statistical Pattern Recognition, Academic Press, 1990.
[24] G.L. Gimel'farb, A.K. Jain, On retrieving textured images from an image database, Pattern Recognition 29 (1996) 1461–1483.
[25] W.N. Gonçalves, J. De Andrade Silva, O.M. Bruno, A rotation invariant face recognition method based on complex network, Lecture Notes in Computer Science, vol. 6419, Springer, Berlin, Heidelberg, 2010.
[26] L.J.V. Gool, P. Dewaele, A. Oosterlinck, Texture analysis anno 1983, Computer Vision, Graphics, and Image Processing 29 (1985) 336–357.
[27] W. Groissboeck, E. Lughofer, S. Thumfart, Associating visual textures with human perceptions using genetic algorithms, Information Sciences 180 (2010) 2065–2084.
[28] Z. Guo, L.Z. 0006, D. Zhang, A completed modeling of local binary pattern operator for texture classification, IEEE Transactions on Image Processing 19 (2010) 1657–1663.
[29] Z. Guo, L. Zhang, D. Zhang, Rotation invariant texture classification using lbp variance (lbpv) with global matching, Pattern Recognition 43 (2010) 706–719.
[30] R.M. Haralick, Statistical and structural approaches to texture, Proceedings of IEEE 67 (1979) 786–804.
[31] Y. Huang, K. Huang, L. Wang, D. Tao, T. Tan, X. Li, Enhanced biologically inspired model, in: CVPR, IEEE Computer Society, 2008, pp. 1–8.
[32] M. Idrissa, M. Acheroy, Texture classification using Gabor filters, Pattern Recognition Letters 23 (2002) 1095–1102.
[33] M.D.J., Random Graphs for Statistical Pattern Recognition, Wiley-Interscience, 2005.
[34] A.K. Jain, F. Farrokhnia, Unsupervised texture segmentation using Gabor filters, Pattern Recognition 24 (1991) 1167–1186.
[35] X. Jin, S. Gupta, K. Mukherjee, A. Ray, Wavelet-based feature extraction using probabilistic finite state automata for pattern classification, Pattern Recognition 44 (2011) 1343–1356.
[36] B. Julesz, Experiments in the visual perception of texture, Scientific American 232 (1975) 34–43.
[37] J.K. Kim, H.W. Park, Statistical textural features for detection of microcalcifications in digitized mammograms, IEEE Transactions on Medical Imaging 18 (1999) 231–238.
[38] U. Knoblich, M. Riesenhuber, D.J. Freedman, E.K. Miller, T. Poggio, Visual categorization: how the monkey brain does it, in: H.H. Bülthoff, S.W. Lee, T. Poggio, C. Wallraven (Eds.), Biologically Motivated Computer Vision, Lecture Notes in Computer Science, vol. 2525, Springer, 2002, pp. 273–281.
[39] B.S. Manjunath, W.Y. Ma, Texture features for browsing and retrieval of image data, IEEE Transactions on Pattern Analysis and Machine Intelligence 18 (1996) 837–842.
[40] D. Marr, Vision: A Computational Investigation into the Human Representation and Processing of Visual Information, Henry Holt and Co., Inc., New York, NY, USA, 1982.
[41] A. Materka, M. Strzelecki, Texture Analysis Methods, A Review, Technical Report, University of Lodz, Institute of Electronics, Brussels, 1998 (COST B11 report).

[42] J.A. Montoya-Zegarra, J.P. Papa, N.J. Leite, R.S. Torres, A.X. Falcpo, Learning how to extract rotation-invariant and scale-invariant features from texture images, EURASIP Journal on Advances in Signal Processing, pp. 1–15.
[43] M.E.J. Newman, The structure and function of complex networks, SIAM Review 45 (2003) 167–256.
[44] I. Ng, T. Tan, J. Kittler, On local linear transform and Gabor filter representation of texture, in: International Conference on Pattern Recognition, pp. 627–631.
[45] T. Ojala, T. Mäenpää, M. Pietikäinen, J. Viertola, J. Kyllönen, S. Huovinen, Outex: New framework for empirical evaluation of texture analysis algorithms, in: International Conference on Pattern Recognition, pp. 701–706.
[46] T. Ojala, M. Pietikäinen, D. Harwood, A comparative study of texture measures with classification based on feature distributions, Pattern Recognition 29 (1996) 51–59.
[47] T. Ojala, M. Pietikäinen, T. Mäenpää, Multiresolution gray-scale and rotation invariant texture classification with local binary patterns, IEEE Transactions on Pattern Analysis and Machine Intelligence 24 (2002) 971–987.
[48] T. Randen, J.H. Husøy, Filtering for texture classification: a comparative study, IEEE Transactions on Pattern Analysis and Machine Intelligence 21 (1999) 291–310.
[49] A. Rapoport, Nets with distance bias, Bulletin of Mathematical Biophysics 13 (1951) 85–91.
[50] A. Rapoport, Spread of information through a population with sociostructural bias: I. Assumption of transitivity, Bulletin of Mathematical Biophysics 15 (1953) 523–533.
[51] A. Rapoport, Contribution to the theory of random and biased nets, Bulletin of Mathematical Biophysics 19 (1957) 257–277.
[52] T. Serre, M. Riesenhuber, J. Louie, T. Poggio, On the role of object-specific features for real world object recognition in biological vision, in: H.H. Bülthoff, S.W. Lee, T. Poggio, C. Wallraven (Eds.), Biologically Motivated Computer Vision, Lecture Notes in Computer Science, vol. 2525, Springer, 2002, pp. 387–397.
[53] D. Song, D. Tao, Biologically inspired feature manifold for scene classification, IEEE Transactions on Image Processing 19 (2010) 174–184.
[54] X. Tan, B. Triggs, Enhanced local texture feature sets for face recognition under difficult lighting conditions, in: S.K. Zhou, W. Zhao, X. Tang, S. Gong (Eds.), Analysis and Modeling of Faces and Gestures, Lecture Notes in Computer Science, vol. 4778, Springer, 2007, pp. 168–182.
[55] M. Tuceryan, A.K. Jain, Texture analysis, in: C.H. Chen, L.F. Pau, P.S.P. Wang (Eds.), Handbook of Pattern Recognition and Computer Vision, World Scientific, 1993, pp. 235–276.
[56] VisTex, Vision Texture Database, 2009.
[57] J.S. Weszka, C.R. Dyer, A. Rosenfeld, A comparative study of texture measures for terrain classification, IEEE Transactions on Systems, Man, and Cybernetics 6 (1976) 269–285.
[58] S. Wuchty, P.F. Stadler, Centers of complex networks, Journal of Theoretical Biology 223 (2003) 45–53.
[59] J. Zhang, T. Tan, Brief review of invariant texture analysis methods, Pattern Recognition 35 (2002) 735–747.
[60] H. Zhou, R. Wang, C. Wang, A novel extended local-binary-pattern operator for texture analysis, Information Sciences 178 (2008) 4314–4325.